

## Collisional-radiative recombination in cold plasmas\*

J. Stevefelt, J. Boulmer, and J-F. Delpech

*Groupe d'Electronique dans les Gaz, Institut d'Electronique Fondamentale, Bât. 220, Université Paris-XI, Centre d'Orsay-91405 Orsay, France*

(Received 3 March 1975)

We have investigated the electron-ion three-body collisional-radiative recombination for electron temperatures below 4000 °K using the Mansbach-Keck rates of electron-impact-induced transitions between hydrogenic energy levels of high principal quantum number. At such temperatures and for a wide range of electron densities, the statistical recombination process is simultaneously governed by collisional and radiative transitions between excited levels near the ionization limit, where many atomic and molecular systems possess a hydrogenic energy-level structure. In order to also take into account radiative transitions, we have numerically solved a system of coupled equations, describing the quasi-steady-state populations of 100 bound levels. These equations are expressed in, and solved for, the first differences between the reduced population densities  $\rho(p)$ , which improves the computing precision and establishes the location of the "bottleneck" in the recombination sequence. Our results are consistent with the following approximation for the collisional-radiative recombination rate coefficient (in  $\text{cm}^3 \text{sec}^{-1}$ ):  $\alpha_{\text{cr}} = 1.55 \times 10^{-10} T^{-0.63} + 6.0 \times 10^{-9} T^{-2.18} [e]^{0.37} + 3.8 \times 10^{-9} T^{-4.5} [e]$ , where the electron temperature  $T$  is in °K and the electron density  $[e]$  is in  $\text{cm}^{-3}$ ; the first and last terms describe purely radiative and collisional recombination, respectively, and the second term results from the complex interplay of collisional and radiative processes. Agreement with experimental data is reasonable.

### I. INTRODUCTION

The process of collisional-radiative recombination has been recognized to play a major role in low-temperature plasmas since 1961 when D'Angelo,<sup>1</sup> Bates and Kingston,<sup>2</sup> and McWhirter<sup>3</sup> independently suggested this complex model. Experimental evidence supports the model for several atomic and diatomic molecular ions such as  $\text{H}^+$  (Cooper and Kunkel<sup>4</sup>),  $\text{He}^+$  and  $\text{He}_2^+$  (numerous articles, for a bibliography see Ref. 5),  $\text{Ne}^+$  and  $\text{Ar}^+$  (Veatch and Oskam<sup>6</sup>),  $\text{Xe}^+$  (Vitols and Oskam<sup>7</sup>), and  $\text{Cs}^+$  (Sayer *et al.*<sup>8</sup>).

As indicated by its very name, coined by Bates *et al.*,<sup>9</sup> this model takes into account both collisional and radiative mechanisms in describing the statistical process of electrons cascading from free continuum states to the fundamental bound level. The rate-limiting step in this process has been localized to energy levels a few  $kT$  below the ionization limit, and at electron temperatures  $T$  below 4000 °K all atoms except for the heaviest (such as Cs) have a hydrogenlike energy-level structure around this "bottleneck." Thus a theory worked out for a cold hydrogen plasma may be expected to be generally valid for the electronic recombination of all atomic ions at low temperatures, as well as for the diatomic molecular ion  $\text{He}_2^+$  (the  $\text{He}_2$  energy levels being hydrogenlike down to 1.5 eV below the ionization limit).

The radiative transition rates for the hydrogen atom have been extensively calculated on the basis

of quantum mechanics, and the results have been reviewed by Bethe and Salpeter.<sup>10</sup> In very tenuous plasmas, recombination will proceed by radiative electron capture, preferentially into the lower quantum levels. This radiative recombination has been theoretically studied by Seaton.<sup>11</sup> In laboratory plasmas, however, energy exchanges through electron collisions are expected to play an important role as well.

Near the ionization limit, i.e., for large principal quantum numbers  $p$ , the correspondence principle leads to the natural assumption that a strictly classical treatment may be applied in computing the electron-impact transition rates. The most recent such computation, which involves a minimum of hypothesis, is due to Mansbach and Keck.<sup>12</sup> They considered a system of one free electron and one bound electron orbiting around a point core, all behaving in accordance with classical laws under influence of the Coulomb interaction, and they used Monte Carlo trajectory calculations to establish the rates of excitation and deexcitation of highly excited states by electron impact. From these rates they derived, in a continuum approximation and neglecting radiation, analytical expressions for the equilibrium population distribution among the excited levels and for the macroscopic rate coefficient for this collisional recombination, valid in the limit of high electron densities.

On a wide range of intermediate electron densities, collisional and radiative processes compete to yield a collisional-radiative recombination rate

which differ markedly from what would be obtained if radiative and collisional recombination were regarded as being simply additive. The present paper is devoted to a detailed computation of excited-states populations and of the recombination rate coefficient in this intermediate range. The method of calculation shall be discussed below.

Recently, Johnson and Hinnov<sup>13</sup> performed similar calculations, using a set of semiempirical cross sections for electron collisional transitions in hydrogen. These cross sections were adjusted to bring experimental and computed population densities into agreement, and they may therefore be considered as relatively accurate for quantum levels up to about  $p=8$ . However, it does not seem

*a priori* justified to extrapolate these cross-section formulas to higher quantum levels, which are of paramount importance for the recombination rate at low temperatures.

## II. FORMULATION OF EQUATIONS

In order to take into account properly both collisional and radiative processes, we have adopted the formalism of Bates *et al.*<sup>9</sup> in calculating the rate of recombination between electrons and hydrogenic ions. Thus an equation is written down for each excited level with principal quantum number  $p$ , describing its quasi-steady-state population  $N(p)$  under influence of the various processes,

$$[e] \sum_{q \neq p} \{K(q, p)N(q) - K(p, q)N(p)\} + [e] \{K(c, p)[X^*] - K(p, c)N(p)\} + \sum_{q > p} A(q, p)N(q) - \sum_{q < p} A(p, q)N(p) + \beta(p)[e][X^*] = 0, \quad (1)$$

where  $[e]$  and  $[X^*]$  are the number densities of free electrons and ions, respectively,  $K(p, q)$  is the rate coefficient for the collisional excitation or de-excitation process

$$X(p) + e \rightarrow X(q) + e, \quad (2)$$

and  $K(c, p)$  and  $K(p, c)$  are the rate coefficients for three-body recombination and its inverse, respectively,

$$X^* + e + e \rightleftharpoons X(p) + e. \quad (3)$$

$A(p, q)$  is the probability for a spontaneous radiative transition,

$$X(p) \rightarrow X(q) + h\nu \quad (4)$$

and  $\beta(p)$  is the rate coefficient for radiative capture into level  $p$ ,

$$X^* + e \rightarrow X(p) + h\nu. \quad (5)$$

$$\sum_{q \neq p} R(p, q)[\rho(q) - \rho(p)] + R(c, p)[1 - \rho(p)] + \sum_{q > p} A(q, p)N_E(q)\rho(q) - \sum_{q < p} A(p, q)N_E(p)\rho(p) + \beta(p)[e][X^*] = 0, \quad (8)$$

where we have introduced the ratio  $\rho(p) = N(p)/N_E(p)$ .

Mansbach and Keck<sup>12</sup> found for the equilibrium transition kernel for hydrogenic energy levels

$$R(p, q) = 120R_0 U^{2.83} (p^{6.66}/q^3) e^{1/\nu q^2}, \quad q > p \quad (9)$$

$$R(c, p) = 60R_0 U^{3.83} p^{6.66},$$

where  $U = kT/\mathcal{R}$ ;  $R_0$  is a characteristic three-body

The principle of detailed balance implies that

$$K(q, p)[e]N_E(q) = K(p, q)[e]N_E(p) = R(p, q), \quad (6)$$

$$K(c, p)[e][X^*] = K(p, c)[e]N_E(p) = R(c, p),$$

where  $N_E(p)$  is the number density of hydrogenic atoms in level  $p$  in local thermodynamic equilibrium (LTE) with the free electrons at temperature  $T$  so that

$$N_E(p) = \left( \frac{h^2}{2\pi m k T} \right)^{3/2} \frac{g(p)}{2g(X^*)} [e][X^*] e^{\mathcal{R}/p^2 k T}, \quad (7)$$

where  $g(p)$  and  $g(X^*)$  are statistical weights of the  $p$ th bound level of the ions in the ground state, respectively, and  $\mathcal{R}$  is the Rydberg constant. Equation (1) may be rewritten in terms of the equilibrium transition kernel  $R(p, q)$ , defined in Eq. (6),

collision rate related to the Thomson radius

$$R_0 = [X^*][e]^2 (kT/m)^{1/2} (e^2/kT)^5. \quad (10)$$

The probability for a spontaneous transition from a hydrogenic level  $q$  to a lower level  $p$  is roughly<sup>10</sup>

$$A(q, p) = 1.6 \times 10^{10} q^{-5.5} \text{ (sec}^{-1}\text{)} \quad (11)$$

for  $p > 1$ . All radiative line transitions to the

ground level  $p=1$  may be omitted because of resonance imprisonment in many experimental situations. The helium molecule  $\text{He}_2$  is an important exception, since its fundamental state is unstable and dissociative.

The rate coefficients  $\beta(p)$  were obtained from Seaton,<sup>11</sup>

$$\beta(p) = 5.197 \times 10^{-14} [X_n S_n(\lambda) / U^{0.5} p] \text{ cm}^3 \text{ sec}^{-1}, \quad (12)$$

where the function  $X_n S_n(\lambda)$ , tabulated by Seaton, as-

$$-\sum_{q=2}^p \left( \sum_{r=1}^{q-1} R(p, r) + \sum_{r=2}^{p-1} A(p, r) N_E(p) - \sum_{r=p+1}^{\infty} A(r, p) N_E(r) \right) \xi(q) + \sum_{q=p+1}^s \left( \sum_{r=q}^{\infty} R(p, r) + R(c, p) + \sum_{r=q}^{\infty} A(r, p) N_E(r) \right) \xi(q) + \beta(p) [e][X^+] = 0, \quad (14)$$

where  $s$  represents the number of bound levels taken into account.

The levels above  $s$  are assumed to be in LTE, so that  $\rho(s)=1$ . Further, as the decaying plasma is far from its final steady state, we put  $\rho(1)=0$ . These lead to the following normalization of the solution for  $\xi(p)$ :

$$\sum_{p=2}^s \xi(p) = 1. \quad (15)$$

The system (14) contains  $s-2$  equations for  $p=2, 3, \dots, s-1$ , which together with the condition (15) yield a unique solution for the  $s-1$  unknowns  $\xi(2), \xi(3), \dots, \xi(s)$ .

The population distribution having been determined, it is possible to evaluate the rate of ion re-

sumes values in the range 0.2–0.9 for  $0.1 < 1/U p^2 < 200$ . Above  $p=16$  the term  $\beta(p)[e][X^+]$  was neglected, as compared with the collisional terms.

Near the ionization limit, the recombination cascade between excited levels is mainly governed by electron collisions, and depends on differences of the form  $\rho(q) - \rho(p)$ , where  $\rho(q)$  and  $\rho(p)$  are both close to unity. To improve the computing precision, we introduced the differences  $\xi(p)$ , defined by

$$\xi(p) = \rho(p) - \rho(p-1). \quad (13)$$

The system of Eq. (8) then transforms into

moval by recombination with electrons. In quasi-steady-state, described by Eq. (1), the number density of atoms in any excited level  $p$  is very much smaller than the ion density, which ensures that

$$\alpha [e][X^+] = -\frac{d}{dt}[X^+] = \frac{d}{dt} N(1). \quad (16)$$

However, in a plasma which is optically thick towards the resonance lines the density of atoms in the quantum level  $p=2$  may become comparable with the free-electron density, and the time derivative of  $N(2)$  should be added to the RHS of Eq. (16). We now obtain two different ways of calculating the recombination coefficient  $\alpha$  defined in Eq. (16),

$$\alpha = \frac{1}{[e][X^+]} \sum_{p=2}^s \left( \sum_{q=1}^{p-1} R(c, q) \right) \xi(p) + \sum_{p=1}^{\infty} \beta(p), \quad (17a)$$

$$\alpha = \frac{1}{[e][X^+]} \left( \sum_{q=3}^{\infty} A(q, 2) N_E(q) \right) \xi(2) + \beta(1) + \beta(2) + \frac{1}{[e][X^+]} \sum_{p=3}^s \left( \sum_{q=p}^s [R(q, 2) + A(q, 2) N_E(q)] \right) \xi(p). \quad (17b)$$

In deriving the second expression we have omitted radiative transitions from the bound levels  $q$  to the fundamental level and neglected the corresponding collisional transitions, as they are about two orders of magnitude less frequent than transitions to the second quantum level.

The system of equations in  $\xi(p)$  was solved in double precision on an IBM 370/168 computer for 98 bound levels. The results of these calculations will be presented and discussed in Sec. III.

### III. COLLISIONAL-RADIATIVE RECOMBINATION COEFFICIENT

From their Monte-Carlo trajectory results on the electron-impact transition rates between various energy levels, Mansbach and Keck<sup>12</sup> derived an analytic distribution function for the bound energies  $\epsilon < 0$

$$\frac{d}{d\epsilon} [\rho(\epsilon)] = -\frac{W/Z^2}{\int_{-\infty}^0 W/Z^2 d\epsilon}, \quad (18)$$

where  $\epsilon = E/kT = -1/Up^2$  and

$$\frac{W}{Z^2} = \frac{(3.83)^2(4.83 - \epsilon)(-\epsilon)^{3.83}e^\epsilon}{30R_0(3.83 - \epsilon)^2}, \quad (19)$$

$$\int_{-\infty}^0 \frac{W}{Z^2} d\epsilon \approx \frac{1.30}{R_0}. \quad (20)$$

In the collisional limit of high electron densities the function

$$\frac{d\rho}{dp} = \frac{2}{up^3} \frac{d\rho}{d\epsilon} \quad (21)$$

provides an excellent representation of our numerical solutions for  $\xi$  shown by the solid line in Fig. 1. The curve has a relatively sharp maximum at an energy  $\epsilon \approx -4.2$ , which may be interpreted as the location of the "bottleneck" for the recombination process. Also, in this limit our calculated values of the recombination rate constant  $\alpha$  are in close agreement with the simple approximate formula given by Mansbach and Keck,

$$\alpha_{\text{coll}} = 3.8 \times 10^{-9} T(^{\circ}\text{K})^{-4.5} [e] \text{ cm}^3 \text{ sec}^{-1}. \quad (22)$$

As a test of internal consistency, it was verified that Eqs. (17a) and (17b) give nearly identical results for the recombination coefficient  $\alpha$ . A correct evaluation of Eq. (17a) requires that a large number of bound energy levels be taken into account. The situation is illustrated by the dashed line in Fig. 1, showing the net collisional recombination rate

$$\alpha_{\text{coll}}(p)/[e] = \{R(c, p)/[e]^2[X^+]\} [1 - \rho(p)] \quad (23)$$

into each energy level  $p$  under conditions close to

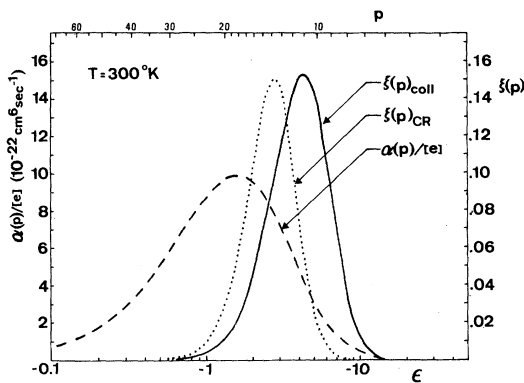


FIG. 1. Numerical solutions for  $\xi(p)$ , obtained at  $T = 300^{\circ}\text{K}$ . Solid curve shows the result for  $[e] = 10^{13} \text{ cm}^{-3}$ , being close to the collisional limit. Dotted curve represents  $\xi(p)$  for  $[e] = 10^9 \text{ cm}^{-3}$ , illustrating the influence of radiation. Dashed curve shows the three-body collisional recombination coefficient  $\alpha(p)/[e]$  into each energy level  $p$ , for  $[e] = 10^{13} \text{ cm}^{-3}$ . Note the important contributions from highly excited levels (large  $p$ ) to the overall recombination rate. Energy scale:  $\epsilon = 1/Up^2$ .

the collisional limit, at  $T = 300^{\circ}\text{K}$ . It may be seen from Eqs. (18) and (19) that for high quantum levels  $[1 - \rho(p)]$  scales as  $p^{-9.66}$ , and hence with  $R(c, p)$  given by Eq. (9), the partial recombination rate  $\alpha(p)$  decreases like  $p^{-3}$ .

For electron densities smaller than  $10^{13} \text{ cm}^{-3}$  transitions to the  $p=2$  level are mainly radiative, and the collisional terms in Eq. (17b) are negligible. The remaining summation in Eq. (17b) has the advantage of being rapidly converging, although this does not remove the necessity of taking into account a relatively large number of bound levels in solving the system of equations. The  $s$  number may here be reduced to about 30–50, well including the "bottleneck" (curve  $\xi$  in Fig. 1).

The existence of a bottleneck in the collisional-radiative recombination sequence was first clearly pointed out by Byron *et al.*<sup>14</sup> They discovered that there exists a pronounced minimum in  $K(p, p^{-1}) \times [e]N_E(p)$ , located at  $p_b \approx (R/3kT)^{1/2}$ . When radiative transitions are added, the location of  $p_b$  is shifted towards higher energies. The minimum serves to limit the net rate of recombination to the rate of deexcitation of the level  $p_b$ .

If the recombination cascade between energy levels were constituted only by collisional transitions with  $\Delta p = \pm 1$ , the quasi-steady-state assumption implies that the rate of recombination be equal to

$$\alpha[e][X^+] = K(p, p-1)[e]N_E(p)\xi(p) \quad (24)$$

taken at any level  $p$ . Hence, in this approximation  $\xi(p)$  will have a maximum where  $K(p, p-1)N_E(p)$  has a minimum. After inclusion of collisional transitions with  $|\Delta p| > 1$  and of radiation, this exact coincidence may not be conserved. However, it is the minimum in the total equilibrium deexcitation rate which causes the transition from  $\rho \approx 1$  to  $\rho \approx 0$  over a relatively limited range of energy levels, and hence this group of levels, for which  $\xi(p)$  is significantly different from zero, must clearly be associated with the bottleneck.

Mansbach and Keck find for the total equilibrium collisional deexcitation rate across an energy  $\epsilon$

$$R_{\text{coll}}(\epsilon) = 7.8R_0(-\epsilon)^{-3.83}e^{-\epsilon}, \quad (25)$$

which has a relatively strong minimum at  $\epsilon_b = -3.83$ . By adding radiative transitions to this crossing rate, we find that the resulting total equilibrium collisional-radiative deexcitation rate has a minimum at an energy  $\epsilon_b$  which satisfies the equation

$$-\epsilon_b - 3.83 + 1.056 \times 10^{-2} \frac{T^{3.75}}{[e]} (-\epsilon_b)^{3.83} (-\epsilon_b - 0.5) = 0. \quad (26)$$

For all electron densities and temperatures con-

sidered, the location of the maximum for  $\xi(p)$  satisfies quite well Eq. (26).

The set of equations in the differences  $\xi(p)$  was solved for a range of electron temperatures 250–4000 °K and electron densities  $10^9$ – $10^{13}$  cm $^{-3}$ . The effect of radiation on the distribution  $\xi(p)$  is demonstrated by the dotted line in Fig. 1, which represents our results for the electron density  $10^9$  cm $^{-3}$  at  $T = 300$  °K. As compared with the collisional limit (solid line) the whole  $\xi$  curve is shifted towards higher quantum levels, resulting in an increased ratio  $\alpha/[e]$  [Eqs. (17)].

In the limit of very low electron densities, Seaton's<sup>11</sup> analysis yields a purely radiative recombination rate which for the electron temperatures considered here can be well represented by the expression

$$\alpha_{\text{rad}} = 1.55 \times 10^{-10} T(^{\circ}\text{K})^{-0.63} \text{cm}^3 \text{sec}^{-1}. \quad (27)$$

These radiative captures occur preferentially into the lower quantum levels [see Eq. (12)], and at the low electron temperatures considered here, they add algebraically to the collisional-radiative mechanisms occurring at the bottleneck. In a wide range of intermediate electron densities, spanning eight decades or more, collisional and radiative processes combine in a complex way so that for the resulting collisional-radiative recombination coefficient  $\alpha_{\text{cr}}$

$$\alpha_{\text{cr}} > \alpha_{\text{coll}} + \alpha_{\text{rad}}. \quad (28)$$

However, by adding one more term to the expression for  $\alpha_{\text{cr}}$ , we find that all our results in the considered range of densities and temperatures can be reproduced to within 10% by the simple formula

$$\alpha_{\text{cr}} = 1.55 \times 10^{-10} T^{-0.63} + 6.0 \times 10^{-9} T^{-2.18} [e]^{0.37} + 3.8 \times 10^{-9} T^{-4.5} [e] \text{cm}^3 \text{sec}^{-1}. \quad (29)$$

Qualitatively, the second term in this expression arises from the shift of the bottleneck position due to radiative transitions, leading to an increased deexcitation rate across the bottleneck. The convenient expression, where  $T$  is in °K, is easily evaluated with pocket calculators and replaces the usual tables for the collisional-radiative recombination coefficient.

The recombination rate coefficient  $\alpha_{\text{cr}}$ , being a function of both  $[e]$  and  $T$ , can be represented by a universal two-dimensional plot with coordinates chosen as

$$\begin{aligned} x &= \log_{10}\{([e] \times 10^{-10})^{-0.258} T\}, \\ y &= \log_{10}\{([e] \times 10^{-10})^{0.163} \alpha_{\text{cr}}\}. \end{aligned} \quad (30)$$

This plot is displayed in Fig. 2 along with the results of four helium afterglow experiments. Most

of the experimental data lie above the dashed line representing the collisional limit given by Eq. (22). Even if the spread in the experimental results is relatively large, they are reasonably well approximated by the solid curve calculated with the full expression (29).

The recombination coefficients calculated by Bates *et al.*<sup>9</sup> and by Johnson and Hinnov<sup>13</sup> cannot be represented by single curves in the diagram of Fig. 2. We have compared in Table I some representative experimental results with the various theoretical predictions. The early measurements by Hinnov and Hirschberg<sup>15</sup> seem to support the calculations of Bates *et al.*, whereas later measurements, in general, yield smaller recombination rates. The computations of Johnson and Hinnov<sup>13</sup> lead to results that are significantly smaller than the measured values, the disagreement being particularly large with respect to the low-temperature results of Collins *et al.*<sup>16</sup> The results of the present calculations are in good overall accordance with the experimental data.

#### IV. CONCLUSIONS

We have combined the recent results of classical Monte Carlo trajectory calculations for the rates

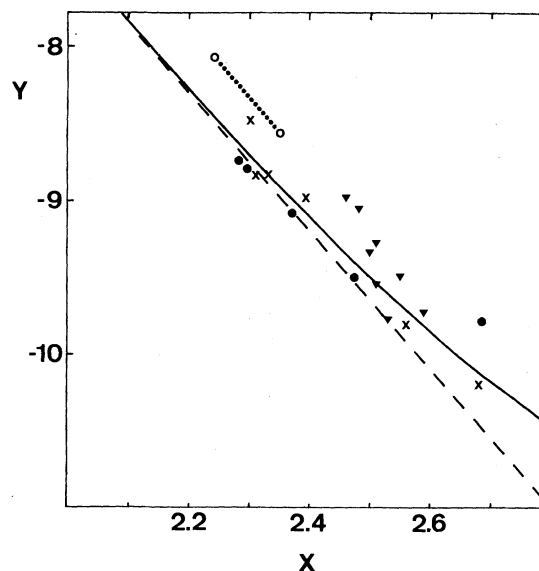


FIG. 2. Universal curve, representing the collisional-radiative recombination coefficient  $\alpha$  as a function of electron density and temperature (solid line). When the coordinates  $X$  and  $Y$  are chosen according to expressions (30), this curve represents well the results of present calculations. For comparison some experimental results are given, transformed by expressions (30), and coded as follows:  $\blacktriangledown$  Hinnov and Hirschberg (Ref. 15),  $\circ \cdots \circ$  Collins *et al.* (Ref. 16),  $\times$  Robben *et al.* (Ref. 17),  $\bullet$  Stevefelt and Robben (Fig. 18). The dashed line represents the collisional limit, Eq. (22).

TABLE I. Selected experimental results compared with various theoretical predictions.

[e] (cm <sup>-3</sup> )	T (°K)	Experiment		Ref.	$\alpha_{\text{theor}}$ (10 <sup>-10</sup> cm <sup>3</sup> sec <sup>-1</sup> )		
		$\alpha$ (10 <sup>-10</sup> cm <sup>3</sup> sec <sup>-1</sup> )			Bates <i>et al.</i>	Johnson and Hinnov	Present
6.2 × 10 <sup>12</sup>	1510	3.6		15	3.3	0.86	1.6
2.3 × 10 <sup>13</sup>	2900	0.53		15	0.57	0.26	0.39
1.0 × 10 <sup>11</sup>	370	29		16	42	3.4	12.4
1.6 × 10 <sup>13</sup>	3250	0.19		17	0.28	0.14	0.21
6.6 × 10 <sup>13</sup>	1975	3.4		17	6.6	2.1	4.0
1.7 × 10 <sup>13</sup>	1275	5.4		18	16.5	3.6	7.7
1.7 × 10 <sup>13</sup>	2000	0.94		18	2.0	0.67	1.2

of electron-impact-induced transitions between highly excited hydrogenic energy levels with the probabilities for radiative deexcitation in a set of coupled rate equations for the various excited levels. The first differences between the Saha decrements for adjacent levels are taken as independent variables, extending the system to include 100 bound energy levels.

In the collisional limit of high electron densities, the computed values of the recombination rate coefficient  $\alpha$  are in good agreement with the simple approximate formula given by Mansbach and Keck, whereas in the low electron-density limit we adopt the rate of radiative recombination calculated by Seaton.<sup>11</sup> In a wide range of intermediate electron densities, spanning eight decades or more, where collisional and radiative processes combine in a

complex way, the resulting collisional-radiative recombination coefficient can be represented by a simple formula containing a third term in addition to the two describing pure collisional and pure radiative recombination, respectively. Inclusion of this term improves the agreement with experimental data obtained in the helium afterglow. This agreement is generally better than what is found for the theories of Bates *et al.*<sup>9</sup> and of Johnson and Hinnov.<sup>13</sup> We believe this to be due to the more correct treatment of collisional transitions between high- $p$  bound energy states, performed by Mansbach and Keck.<sup>12</sup> An independent measurement of the electron-impact transition rates between these energy states, which are in general close to Saha equilibrium with each other and with the free electrons, would be highly desirable.

\*Work partly supported by Direction des Recherches et Moyens d'Essais under contract No. 73-34-380.

<sup>1</sup>N. D'Angelo, *Phys. Rev.* **121**, 505 (1961).

<sup>2</sup>D. R. Bates and A. E. Kingston, *Nature* **189**, 652 (1961).

<sup>3</sup>R. W. P. McWhirter, *Nature* **190**, 902 (1961).

<sup>4</sup>W. S. Cooper and W. P. Kunkel, *Phys. Rev. A* **138**, 1022 (1965).

<sup>5</sup>J.-F. Delpech, J. Boulmer, and J. Stevefelt, in *Advances in Electronics and Electron Physics*, edited by L. Marton (Academic, New York, 1975), Vol. 39.

<sup>6</sup>G. E. Veatch and H. J. Oskam, *Phys. Rev. A* **1**, 1498 (1970); **2**, 1422 (1970).

<sup>7</sup>A. P. Vitols and H. J. Oskam, *Phys. Rev. A* **8**, 3211 (1973).

<sup>8</sup>B. Sayer, J.-C. Jeannet, J. Lozingot, and J. Berlande, *Phys. Rev. A* **8**, 3012 (1973).

<sup>9</sup>D. R. Bates, A. E. Kingston, and R. W. P. McWhirter, *Proc. R. Soc. A* **267**, 297 (1962); **270**, 155 (1962).

<sup>10</sup>H. A. Bethe and E. E. Salpeter, *Quantum Mechanics of One- and Two-Electron Atoms* (Academic, New York, 1957), Table 15, p. 266.

<sup>11</sup>M. J. Seaton, *Mon. Not. R. Astron. Soc.* **119**, 81 (1959).

<sup>12</sup>P. Mansbach and J. Keck, *Phys. Rev.* **181**, 275 (1969).

<sup>13</sup>L. C. Johnson and E. Hinnov, *J. Quant. Spectrosc. Radiat. Transfer* **13**, 333 (1973).

<sup>14</sup>S. Byron, R. C. Stabler, and P. I. Bortz, *Phys. Rev. Lett.* **8**, 376 (1962).

<sup>15</sup>E. Hinnov and J. G. Hirschberg, *Phys. Rev.* **125**, 795 (1962).

<sup>16</sup>C. B. Collins, H. S. Hicks, W. E. Wells, and R. Burton, *Phys. Rev. A* **6**, 1545 (1972).

<sup>17</sup>F. Robben, W. B. Kunkel, and L. Talbot, *Phys. Rev.* **132**, 2363 (1963).

<sup>18</sup>J. Stevefelt and F. Robben, *Phys. Rev. A* **5**, 1502 (1972).